IJPSR (2021), Volume 12, Issue 3 **(Research Article)**

INTERNATIONAL JOURNAL OF PHARMACEUTICAL SCIENCES AND RESEARCH

Received on 17 March 2020; received in revised form, 29 June 2020; accepted, 16 July 2020; published 01 March 2021

DOCKING - BASED VIRTUAL SCREENING OF LIPINSKI COMPLIANT 2 -ARYLQUINAZOLIN - 4 - ONE DERIVATIVES: A MOMENTUM TO THE DISCOVERY OF NOVEL EGFR INHIBITORS

P. K. Arora [*1] S. Kumar [2] and S. K. Bansal [3]

Faculty of Pharmacy [1], IFTM University, School of Pharmaceutical Sciences [2], Moradabad - 244001, Uttar Pradesh, India.
Ram-Eesh Institute of Vocational and Technical Education, Greater Noida - 201310, Uttar Pradesh, India

Keywords:

Molecular modeling, Anticancer agents, Computational chemistry, Drug design, Docking, EGFR inhibitors

Correspondence to Author:
P. K. Arora

Faculty of Pharmacy, IFTM University, Moradabad - 244001, Uttar Pradesh, India.

E-mail: procarora@gmail.com

ABSTRACT: The epidermal growth factor receptor (EGFR), which is a potential anticancer drug target, is over-expressed in non-small-cell lung cancer (NSCLC). The present study is an attempt to explore the human EGFR (protein data bank code: 1M17) inhibition potential of Lipinski compliant compounds possessing 2-arylquinazoli-4-one scaffold with chalcone structural motif; by docking analysis, using Auto Dock 4.0 and Discovery Studio Visualizer. Docking experiments were validated by docking the reported co-crystallized erlotinib confermer at the active site of a target protein. The root means square deviation (RMSD) calculated for the docked co-crystallized confermer by using UCSF chimera was 0.989Ao. Five compounds C21, C42, C47, C10, and C46, were found as the most potent *in-silico* EGFR inhibitors and their free energy of binding (BE) came in the range of -45.56 kJ/mol to -41.25 kJ/mol. Absorption and toxicity predictions of the compounds were done using ad met SAR, an online prediction tool. The BE of the reference compound afatinib was found to be -32.72 kJ/mol. The understanding of protein-legend interactions would give accurate guidance for the rapid development of low molecular weight EGFR inhibitors.

INTRODUCTION: Docking-based drug design by using the structure of target protein remains one of the most rational and speedy approaches in drug discovery paradigms. The knowledge about the amino acid residues interacting with the specific groups of the chemical entity leads to proposals for the synthesis of the new highly potent chemical entities [1]. In recent years, virtual screening by computational methods has become an essential part of drug discovery projects [2]. During the past decade, profound research has initiated a new era of cancer treatment involving drugs with novel molecular targets.

QUICK RESPONSE CODE

DOI: 10.13040/IJPSR.0975-8232.12(3).1699-12

This article can be accessed online on www.ijpsr.com

DOI link: http://dx.doi.org/10.13040/IJPSR.0975-8232.12(3).1699-12

Among all types of cancer, lung cancer is the most commonly diagnosed cancer, there have been huge efforts for treatment advancements over the last 20 years, but still, poor prognosis persists for patients with advanced non-small cell lung cancer (NSCLC) [3]. One of the main reasons behind the poor prognosis of NSCLC is EGFR overexpression [4].

Clinical trials demonstrated that erlotinib and afatinib have greater efficacy regarding proliferation free survival (PFS) and response rate than conventional chemotherapy (*viz;* cisplatin, carboplatin, *etc*.), and as a result, these drugs were approved by the US Food and Drug Administration (FDA) [5, 6]. As compared to conventional chemotherapy (*viz*; cisplatin, carboplatin, *etc*.), the toxicities associated with low molecular weight EGFR tyrosine kinase inhibitors are more tolerable (*viz*; rash and diarrhea and rarely interstitial lung disease) [7].

The comparative clinical studies between erlotinib and afatinib reported the superiority of afatinib over erlotinib regarding proliferation-free survival and overall survival in the advanced NSCLC patients, but the incidence of treatment-related diarrhea and stomatitis was greater with afatinib than that of erlotinib [8, 9]. With the objective of searching new better low molecular weight EGFR tyrosine kinase inhibitors with superior potency, 47 Lipinski compliant 2-arylquinazolin-4-one incur-porated chalcones were designed, their absorption capability through the human intestine and blood-brain barrier (BBB), and their toxicity (mutagen city and carcinogenicity) and LD_{50}, were predicted using ad met SAR, an online prediction tool. The compounds were docked to evaluate their EGFR inhibition potential in terms of free binding energy (BE) and Inhibition Constant (KI). The results of these studies will give a momentum to discover novel low molecular weight EGFR tyrosine kinase inhibitors with distinguished virtues over the existing ones.

MATERIALS AND METHOD:

Sources and Softwares: In the present docking study, X-ray diffraction 3D crystal structure of EGFR from protein data bank (https:// www.rcsb.org/, PDB ID: 1M17) was used as a target protein [10]. The open-source software tools used were Discovery Studio Visualizer 2017 R2 (Dassault Systèmes BIOVIA, https://www.3 dsbiovia.com), Marvin Sketch version 18.23 (Chemaxon Ltd; http://www.Chemaxon.com), Auto Dock 4.0 MGL tools (The Scripps Research Institute, Molecular Graphics Laboratory, 10550 North Torrey Pines Road, CA, 92037), UCSF chimera (https://www.cgl.ucsf.edu/chimera). The online web tools used were swiss ADME (http://www.swissadme.ch), and ad met SAR (http://lmmd.ecust.edu.cn/admetsar1). All the docking experiments were done on a 1.7 GHz Intel (R) core i5 system with 3.8 GB of RAM and a Red Hat Enterprise Linux 6.6 operating system.

Data Set of Ligands: A data set of ligands was prepared and screened for the Lipinski drug-likeness by using the Swiss ADME online server. Among them, 47 ligands complied the Lipinski rule of five; hence they constituted the data set [11, 12].

Absorption and Toxicity Prediction: Absorption capability of 47 ligands through the human intestine and blood-brain barrier (BBB), and their toxicity (mutagenicity and carcinogenicity) and LD_{50}, were predicted using ad met SAR, an online prediction tool.

Protein Preparation: It consists of several steps; firstly, the crystal structure of Human epidermal growth factor receptor (EGFR) PDB code 1M17 complexed with erlotinib was downloaded in .pdb format from protein data bank (PDB; http://www.rcsb.org/pdb) as shown in **Fig. 1A** and loaded to Discovery Studio Visualizer for the removal of water molecules, non bonded atoms and co-crystallized erlotinib. The refined 3D crystal structure **Fig. 1B** of 1 m17 protein was made ready for auto grid computing and docking experiments using Auto Dock 4.0 MGL tools by adding polar hydrogen, merging non-polar hydrogen, and adding Kollman charges than was saved in. pdbqt format [13, 14].

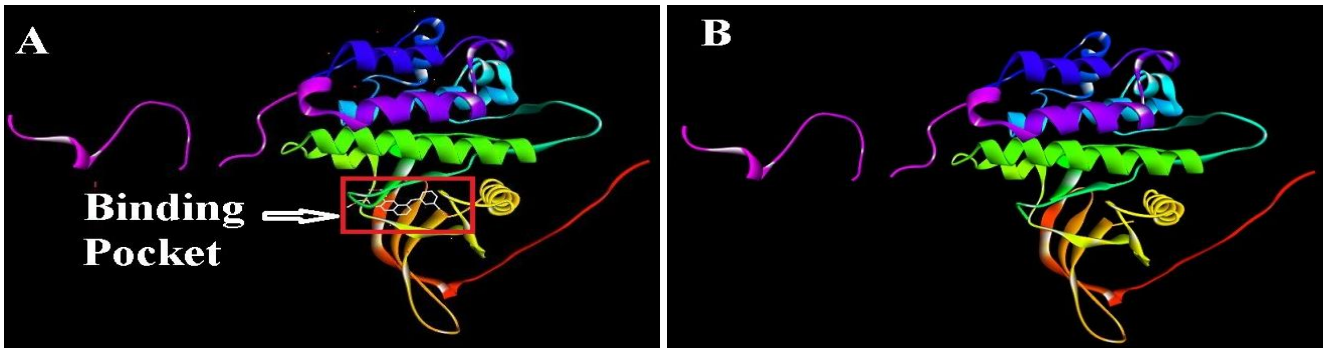

FIG. 1: (A) EGFR (1M17) COMPLEXED WITH ERLOTINIB (B) EGFR (1M17)

Ligand preparation: MarvinSketch version 18.23 was used to draw the 2D structures and then subsequently to 3D structures; of all the 47 ligands, explicit hydrogen was added, the geometry of ligands were then cleaned, and energy minimization of the ligands was done in an

MMFF94 force field by gradient optimization function of Marvin Sketch. The ligand 3D structures were saved in. pdb format. The ligands were prepared as per the protocol mentioned in autodock tutorial (http://autodock.scripps.edu). The ligand structure (.pdb file) was opened in Auto Dock Tools. All atoms of the ligand were assigned AD4 type, polar hydrogen was added, and non-polar hydrogen was merged, Gasteiger charges were added, then ligand structure was saved in .pdbqt format for autogrid computing and docking experiments [13, 14].

Validation of Docking Experiment: The co-crystallized conformer of erlotinib was separated from the EGFR crystal structure using Discovery Studio Visualizer. The separated co-crystallized conformer was prepared as per the protocol of ligand preparation and then was re-docked with the prepared target protein 1M17 under different grid parameters and docking parameters to get the docked pose having minimum RMSD value with respect to the reported erlotinib co-crystallized conformer. The set of grid and docking parameters that had given the least RMSD value were selected for performing docking experiments. The RMSD values were calculated by using UCSF chimera.

Molecular Docking Studies: The validated grid parameters and docking parameters were employed for autogrid computing and docking studies. In preparing the grid parameter file (.gpf), 3D grid box was placed at the centre of the target protein (PDB: 1M17); along x, y, and z-axis of the 3D grid box 100 points were selected, a grid spacing of 0.375 A ° (roughly a quarter of the length of a carbon-carbon single bond) was used. By using .gpf file of the ligand understudy, Autogrid 4.0 was run to generate. glg files having grid maps of interaction energies of various atom types present in the ligand. In preparing the docking parameter file (.dpf), 50 independent runs (each run was comprised of an initial population of 150 individuals), with step sizes of 0.2 A° for translations and 5 A° for orientations and torsions, a maximum number of 2,500,000 energy evaluations, the maximum number of generations of 27,000, an elitism value (number of top individuals that automatically survive) of 1 and a number of active torsion of 9 was used. By using .dpf file of the ligand, Autodock4.0 was run to generate .dlg file.

Docking Analysis, Visualization of Docked Pose and Interactions: Of the three different search algorithms offered by Autodock 4.0, the Lamarckian genetic algorithm (LGA) based on the optimization algorithm was used. The free energy of binding (BE) and inhibition constant (KI) of ligands were obtained from the. dlg files of the respective ligands. The complex between the best-fit ligand conformer and the target protein (1M17), was opened in Discovery Studio Visualizer to observe predicted binding pose of the ligand and its interactions with the target macromolecule (1M17).

RESULTS AND DISCUSSION: There are a number of currently available drugs that are based on quinazolinone scaffold (*viz*; raltitrexed for large intestine cancer treatment, methaqualone has sedative effects), *in-vitro* EGFR inhibition assay on certain quinazolinone and quinazoline derivatives have been carried out, and some of them are reported as potent EGFR inhibitors [15-17]. The immense therapeutic potential of the quinazolinone scaffold motivated the present research to choose quinazolinone as a scaffold in designing novel EGFR inhibitors.

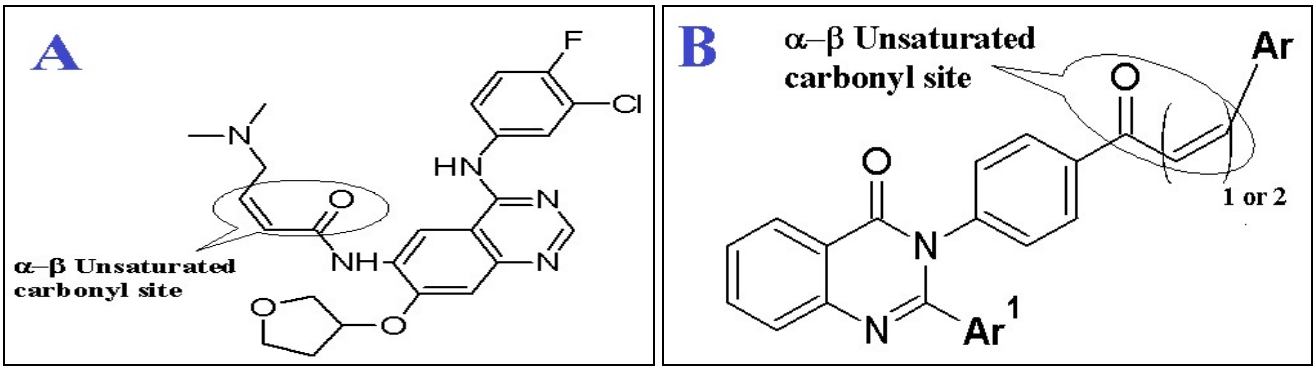

FIG. 2: (A) AFATINIB (B) 2-ARYLQUINAZOLIN-4-ONE DERIVATIVES

It is reported that afatinib interacts with the target EGFR by Michael addition reaction [18]. The presence of carbon-carbon α-β unsaturated carbonyl site in afatinib **Fig. 2A** makes it a good substrate for Michael addition reaction, keeping this fact in mind quinazolinone derivatives were designed to have carbon-carbon α-β unsaturated carbonyl site **Fig. 2B** and to follow the Lipinski rule of drug-likeness. There are many reports which justify the incorporation of chalcone structural motif, for the development of new anticancer drugs [19, 20]. Recently, 1, 4 - dihydroindeno [1, 2 - c] pyrazole chalcones, 1, 3, 4 - oxadiazole / chalcone hybrids and thienoquinoline-2-carboxamide chalcone derivatives have been reported as significant EGFR inhibitors [21-23]. In the present work, before performing docking experiments, 47 Lipinski compliant ligands were analyzed for human intestinal absorption (HIA), blood-brain barrier absorption (BBBA), toxicity potential (mutagenicity and carcinogenicity), and their lethal dose (LD_{50}), using ad met SAR. The results are listed in **Table 1**. The absorption through BBB and the human intestine is expressed in terms of probability. All the ligands in the data set showed good HIA and BBB absorption. None of the compounds were carcinogenic, and except C41, all the other compounds were non-mutagenic.

TABLE 1: ABSORPTION, TOXICITY AND LD_{50} ANALYSIS OF 2-ARYLQUINAZOLIN-4-ONE INCORPORATED CHALCONES

2-Arylquinazolin-4-one incorporated chalcones:

(1) 3-{4-[3-(aryl)prop-2-enoyl]phenyl}-2- phenyl-3,4-dihydroquinazolin-4-one derivatives

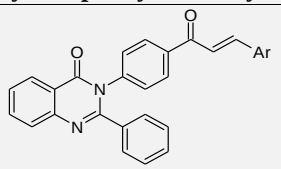

Compound Code	Ar	BBBA	HIA	AMES toxicity (for Mutagenicity)	Carcinogenicity	LD_{50} Mol/kg
C1	Phenyl	0.9954	0.9974	No	No	2.8133
C2	4-Chlorophenyl	0.9899	1	No	No	2.4666
C3	4-Hydroxyphenyl	0.974	0.9965	No	No	2.9129
C4	4-Methoxyphenyl	0.9853	1	No	No	2.6275
C5	4-Hydroxy-3-methoxyphenyl	0.9052	0.9795	No	No	2.6213
C6	3,4-Dimethoxyphenyl	0.958	0.9924	No	No	2.5312
C7	4-Hydroxy-3,5-dimethoxyphenyl	0.8899	0.9777	No	No	2.6491
C8	3,4,5-Trimethoxyphenyl	0.9621	0.9932	No	No	2.6031
C9	Furan-2-yl	0.9958	1	No	No	2.5116
C10	Naphthalen-1-yl	0.9954	0.9974	No	No	2.8133
C11	Pyridin-3-yl	0.9954	0.9974	No	No	2.8133

(2) 3-{4-[3-(aryl)prop-2-enoyl]phenyl}-2-(furan-2-yl)-3,4-dihydroquinazolin-4-one derivatives

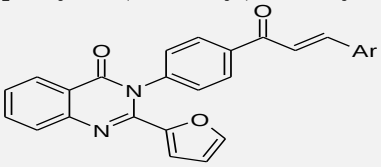

Compound Code	Ar	BBBA	HIA	AMES toxicity (for Mutagenicity)	Carcinogenicity	LD_{50} Mol/kg
C1	Phenyl	0.9954	0.9974	No	No	2.8133
C2	4-Chlorophenyl	0.9899	1	No	No	2.4666
C3	4-Hydroxyphenyl	0.974	0.9965	No	No	2.9129
C4	4-Methoxyphenyl	0.9853	1	No	No	2.6275
C5	4-Hydroxy-3-methoxyphenyl	0.9052	0.9795	No	No	2.6213
C6	3,4-Dimethoxyphenyl	0.958	0.9924	No	No	2.5312

C7	4-Hydroxy-3,5-dimethoxyphenyl	0.8899	0.9777	No	No	2.6491
C8	3,4,5-Trimethoxyphenyl	0.9621	0.9932	No	No	2.6031
C9	Furan-2-yl	0.9958	1	No	No	2.5116
C10	Naphthalen-1-yl	0.9954	0.9974	No	No	2.8133
C11	Pyridin-3-yl	0.9954	0.9974	No	No	2.8133

(2) 3-{4-[3-(aryl)prop-2-enoyl]phenyl}-2-(furan-2-yl)-3,4-dihydroquinazolin-4-one derivatives

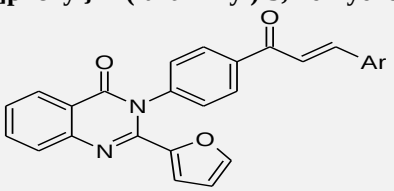

Compound Code	Ar	BBBA	HIA	AMES toxicity (For Mutagenicity)	Carcinogenicity	LD_{50} Mol/kg
C12	Phenyl	0.9933	1	No	No	2.5319
C13	4-Chlorophenyl	0.9877	1	No	No	2.3181
C14	4-Hydroxyphenyl	0.9543	0.9954	No	No	2.6049
C15	4-Methoxyphenyl	0.9648	1	No	No	2.4632
C16	4-Hydroxy-3-methoxyphenyl	0.887	0.9917	No	No	2.5355
C17	3,4-Dimethoxyphenyl	0.9457	0.9969	No	No	2.4176
C18	4-Hydroxy-3,5-dimethoxyphenyl	0.8525	0.9909	No	No	2.5596
C19	3,4,5-Trimethoxyphenyl	0.9434	0.9973	No	No	2.4794
C20	Furan-2-yl	0.9867	0.9968	No	No	2.3934
C21	Naphthalen-1-yl	0.9933	1	No	No	2.5319
C22	Pyridin-3-yl	0.9933	1	No	No	2.5319

(3) 3-{4-[3-(aryl)prop-2-enoyl]phenyl}-2-(4-chlorophenyl)-3,4-dihydroquinazolin-4-one derivatives

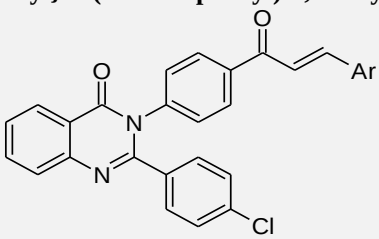

Compound Code	Ar	BBBA	HIA	AMES toxicity (For Mutagenicity)	Carcinogenicity	LD_{50} Mol/kg
C23	Phenyl	0.9899	1	No	No	2.4666
C24	4-Chlorophenyl	0.9899	1	No	No	2.4666
C25	4-Hydroxyphenyl	0.9461	0.9971	No	No	2.5139
C26	4-Methoxyphenyl	0.9766	1	No	No	2.3969
C27	4-Hydroxy-3-methoxyphenyl	0.8646	0.9827	No	No	2.4403
C28	3,4-Dimethoxyphenyl	0.9391	0.9936	No	No	2.3644
C29	4-Hydroxy-3,5-dimethoxyphenyl	0.8369	0.9813	No	No	2.4909
C30	3,4,5-Trimethoxyphenyl	0.9426	0.9943	No	No	2.4031
C31	Furan-2-yl	0.9914	1	No	No	2.3295
C32	Pyridin-3-yl	0.9899	1	No	No	2.4666

(4) 3-{4-[3-(aryl)prop-2-enoyl]phenyl}-2-(4-methoxyphenyl)-3,4-dihydroquinazolin-4-one derivatives

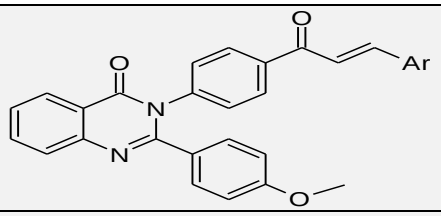

Compound Code	Ar	BBBA	HIA	AMES toxicity (for Mutagenicity)	Carcinogenicity	LD_{50} Mol/kg
C33	Phenyl	0.9853	1	No	No	2.6275
C34	4-Chlorophenyl	0.9766	1	No	No	2.3969
C35	4-Hydroxyphenyl	0.9143	0.9826	No	No	2.6346
C36	4-Methoxyphenyl	0.9619	0.9936	No	No	2.517
C37	4-Hydroxy-3-methoxyphenyl	0.8803	0.9727	No	No	2.6103
C38	3,4-Dimethoxyphenyl	0.9578	0.9917	No	No	2.5289
C39	4-Hydroxy-3,5-dimethoxyphenyl	0.8917	0.9755	No	No	2.6507
C40	3,4,5-Trimethoxyphenyl	0.9621	0.9932	No	No	2.6031
C41	Furan-2-yl	0.9803	1	Yes	No	2.4503
C42	Naphthalen-1-yl	0.9853	1	No	No	2.6275
C43	Pyridin-3-yl	0.9853	1	No	No	2.6275

(5) 2-aryl-3-{4-[5-phenylpenta-2,4-dienoyl]phenyl}-3,4-dihydroquinazolin-4-one derivatives

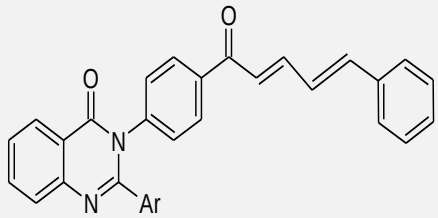

Compound Code	Ar	BBBA	HIA	AMES toxicity (for Mutagenicity)	Carcinogenicity	LD_{50} Mol/kg
C44	Phenyl	0.9954	0.9974	No	No	2.8133
C45	Furan-2-yl	0.9933	1	No	No	2.5319
C46	4-Chlorophenyl	0.9899	1	No	No	2.4666
C47	4-Methoxyphenyl	0.9853	1	No	No	2.6275
Afatinib	-	0.8717	1	No	No	2.5643

Docking Validation: The reported co-crystallized confermer of erlotinib with target EGFR (1M17) was redocked and the minimum RMSD obtained between the co-crystallized confermer and its redocked pose was 0.989A^{o} as shown in **Fig. 3**, which implies that the used grid parameters and docking parameters had successfully generated the docking pose which is very close to the reported co-crystallized confermer [10].

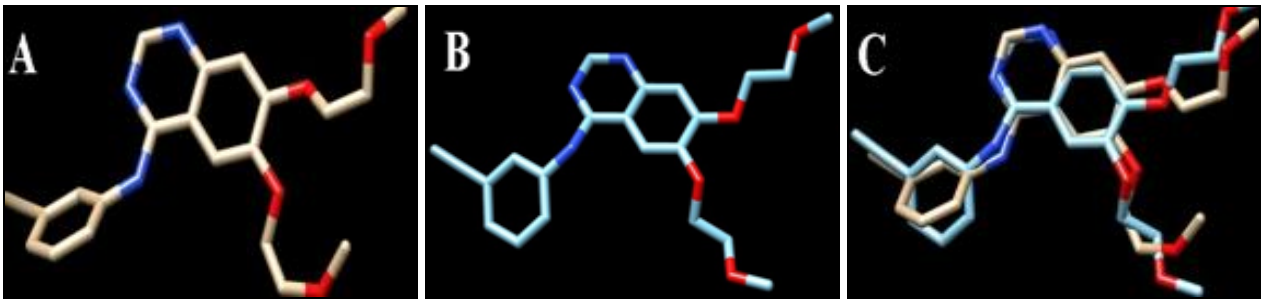

FIG. 3: (A) CO-CRYSTALLIZED ERLOTINIB CONFERMER (B) REDOCKED POSE ERLOTINIB CO-CRYSTALLIZED CONFERMER (C) SUPERIMPOSED CO-CRYSTALLIZED ERLOTINIB CONFERMER AND ITS REDOCKED POSE

Molecular Docking Results: All the docked compounds binded at the reported binding pocket of EGFR (1M17) **Fig. 4** that ensures their ligand efficiency and the accuracy of the docking experiments. The docked ligands are ranked on the basis of free binding energy (BE) and inhibition constant (KI). The interactions were observed by using Discovery Studio Visualizer. The docking analysis is tabulated in **Table 2**. Afatinib **Fig. 5** forms conventional hydrogen bonds, with GLN767 and ASP831, Pi-Sigma interactions with LEU694 and LEU820, Pi-Alkyl interactions with ALA719 and VAL702 & Alkyl interactions with LYS721, MET742, and LEU768.

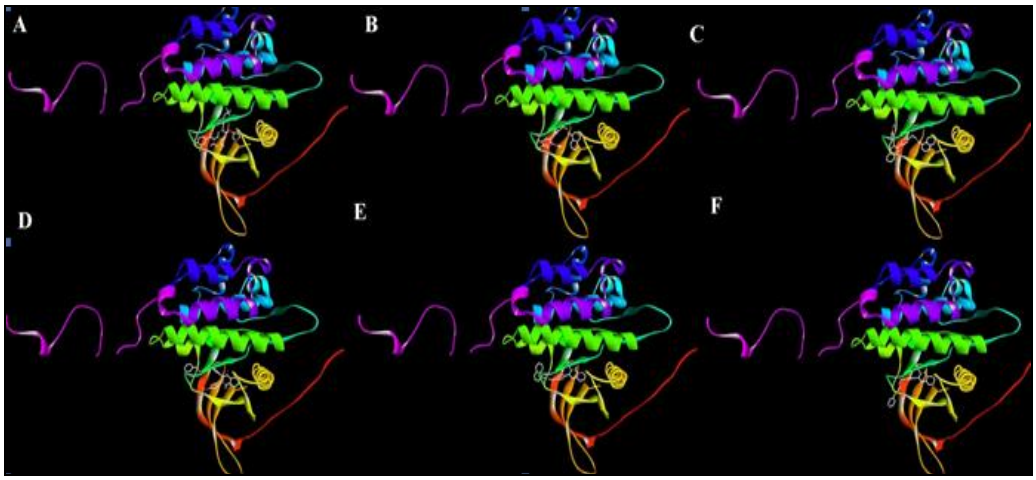

FIG. 4: AFATINIB AND FIVE MOST POTENT LIGANDS IN THE BINDING POCKET OF EGFR (A) AFATINIB (B) C21 (C) C42 (D) C47 (E) C10 (F) C46

TABLE 2: MOLECULAR DOCKING ANALYSIS

S. no.	Compound Code	BE kJ/mol	KI nmol	Docking Rank	No. of H Bonds	H Bonds Interaction Residues and (Bond Distance in A^0)	Other Interaction Residues (Polar and Non-polar)	No. of Interacting Residues
1	C1	-37.91	227.77	31	1	ASP831(1.68)	LEU820, MET742, LYS721, VAL702, PRO770, LEU768, LEU694, CYS773	9
2	C2	-39.75	108.09	9	1	ASP831(2.10)	LEU694, PRO770, LYS704 ,LEU768, LEU820, VAL702, LYS721, MET742, GLY772	10
3	C3	-37.61	258.71	34	1	LYS721(2.07)	CYS773, MET742, ASP831, LEU820, VAL702, ALA719, THR766, LEU764	9
4	C4	-39.54	118	12	1	ASP831(1.77)	MET742, LYS721, LEU820, VAL702, GLY772, CYS773, LEU694	8
5	C5	-37.66	253.51	32	1	ASP831(2.24)	LYS721, MET742, VAL702, LEU820, LEU694, LEU768, PRO770	8
6	C6	-37.03	327.72	39	1	CYS773(2.63)	PRO770, LEU768, LEU694, ASP831, LYS721, MET742, VAL702, LEU820	9
7	C7	-37.61	255.6	33	0	-	ASP776, HIS781, PRO770, VAL702, ALA719, LEU820, LEU694	7
8	C8	-36.61	386.32	42	0	-	PRO770, VAL702, ALA719, LEU820, LEU694	5

9	C9	-37.28	292.02	35	1	ASP831(1.81)	LYS721, MET742, LEU820, LEU768, PRO770, MET769, LYS704, LEU694, VAL702, CYS773	11
10	C10	-41.84	46.97	4	1	ASP831(2.06)	VAL702, LEU694, CYS773, LEU820, MET742	6
11	C11	-37.20	302.47	36	1	ASP831(2.41)	LYS721, VAL702, LEU768, PRO770, LYS704, LEU694, LEU820, CYS773	9
12	C12	-36.48	405.34	45	1	MET769(2.08)	GLU780, TYR777, LEU694, VAL702, ALA719, LEU820	7
13	C13	-38.49	179.06	23	1	ASP831(2.18)	MET742, LYS721, VAL702, LEU820, LEU768, LYS704, PRO770, LEU694	9
14	C14	-38.45	183.6	25	2	ASP831(1.92), LYS704(2.82)	GLY772, LYS721, LEU820, LEU768, LEU694, CYS773, VAL702	9
15	C15	-37.91	227.53	30	0	-	GLY772, HIS781, GLU780, LEU694, VAL702, LEU820, ALA719, MET769, CYS773	9
16	C16	-36.61	386.65	43	1	ASP831(1.96)	PHE771, TYR777, MET742, VAL702, LEU694, CYS773, LEU820	8
17	C17	-36.61	388.66	44	0	-	GLY772, HIS781, CYS773, LEU694, GLU780, VAL702, LEU820, ALA719, PRO770	9
18	C18	-37.07	320.52	37	2	MET769(2.68), THR830(2.61)	GLN767, THR766, CYS751, LEU820, ALA719, VAL702, LEU694	9
19	C19	-38.07	212.23	29	1	CYS773(2.36)	GLY772, ARG817, LEU694, LYS704, ,LYS721, ALA719, VAL702, LEU820, ASP831	10
20	C20	-37.03	325.67	38	1	ASP831(1.99)	GLY772, ARG817, LYS721, VAL702, LYS704, LEU768, PRO770, LEU820, LEU694	10
21.	C21	-45.56	10.41	1	2	MET769(1.98, 2.49)	GLN767, LEU820, MET742, LYS721, ALA719, VAL702, LEU694	8
22	C22	-38.66	168.69	21	2	MET769(2.01), GLU738(2.04)	GLN767, ASP831, ALA719, LEU768, LEU820, MET742, LEU694, LYS721, VAL702	11
23	C23	-39.75	109.6	10	1	ASP831(2.12)	GLY772, LYS721, VAL702, LYS704, LEU768, LEU694, LEU820, PRO770,	9
24	C24	-40.21	89.95	7	1	ASP831(2.02)	ARG817, HIS781, LYS721, MET742,	10

							LEU820, VAL702, TYR777, LEU694, CYS773	
25	C25	-38.79	159.47	18	1	ASP831(2.31)	VAL702, LEU820, LEU694, LEU768, LYS721, LYS704, ARG817	8
26	C26	-40.71	74.35	6	1	LYS721(2.21)	ASP813, ASP831, ARG817, LEU820, LEU694, ALA719, VAL702, LEU764, MET742	10
27	C27	-39.04	143.94	16	1	ASP831(2.05)	PHE771, TYR777, ARG817, CYS773, MET742, VAL702, LEU820, ALA719	9
28.	C28	-38.45	183.28	24	0	-	PRO770, PHE699, ASP831, MET742, LYS721, LEU820, VAL702, LEU694, LEU768	9
29	C29	-38.95	150.88	17	1	LYS721(2.31)	ASP831, ALA719, ASP813, ARG817, LEU694, LEU820, VAL702	8
30	C30	-36.90	345.51	40	0	-	ASP813, ASP831, LYS721, CYS773, GLU738, VAL702, LEU820, LEU694	8
31	C31	-38.70	165.09	20	1	CYS773(1.94)	ASP776, LEU820, ASP831, LYS721, LEU764, MET742, VAL702, ALA719	9
32	C32	-38.62	170.64	22	1	ASP831(2.03)	LYS721, MET742, LEU820, VAL702, LYS704, PRO770, MET769, LEU768, LEU694, CYS773, ARG817	12
33	C33	-39.37	125.9	14	1	MET769 (2.38)	ALA719, LEU820, LEU768, LEU694, VAL702, LYS721, MET742	8
34	C34	-39.25	132.74	15	1	ASP831(1.92)	TYR777, HIS781, LEU820, LYS721, MET742, VAL702, CYS773	8
35	C35	-38.20	201.42	26	2	ASP813(1.87), LYS721(2.10)	MET769, LEU820, LEU694, VAL702, ALA719, ASP831, ARG817	9
36	C36	-39.66	113.02	11	1	ASP831(1.84)	ARG817, LYS721, MET742, LEU694, VAL702, LEU820, GLY272, CYS773	9
37	C37	-38.74	161.77	19	1	ASP831(1.81)	PRO770, CYS773, LYS721, MET742, LEU820, VAL702, LYS704, LEU768, MET769, LEU694	11
38	C38	-36.86	347.34	41	1	ASP831(1.91)	LYS721, MET742, VAL702, LEU820, LEU694, LYS704, LEU768, CYS773	9
39	C39	-38.07	212.03	28	1	MET769(2.77)	PRO770, HIS781, LEU694, VAL702, LEU820, ALA719	7

40	C40	-36.32	431.97	47	0	-	PRO770, GLU780, ASP776, PHE771, VAL702, MET769, ALA719, LEU820, LEU694	9
41	C41	-36.36	423.39	46	1	ASP831(1.96)	PRO770, CYS773, MET742, LEU820, VAL702, LEU694, LYS704, LEU768	9
42	C42	-43.81	21.16	2	1	MET769 (2.9)	ASP776, LEU820, VAL702, MET742, LYS721, ALA719, PRO770, LEU768, LYS704, LEU694	11
43	C43	-38.12	211.8	27	2	ASP813(1.77), LYS721(2.12)	ASN818, LEU820, VAL702, LEU694, ALA719, CYS773, ASP831	9
44	C44	-39.79	107.16	8	1	ASP831 (2.02)	LYS721, MET742, VAL702, LEU820, LEU694, PRO770, LYS704, LEU768	9
45	C45	-39.46	122.43	13	1	ASP831(1.95)	MET742, LYS721, VAL702, LEU820, LEU694, LEU768, LYS704	8
46	C46	-41.25	59.39	5	1	ASP831 (1.87)	CYS773, ARG817, LYS704, PRO770, LEU768, LEU694, VAL702, LEU820, LYS721, MET742	11
47	C47	-42.89	30.85	3	2	LYS721(2.15), MET769 (1.84)	ASP831, VAL702, LEU764, MET742, LEU820, ALA719, CYS773, GLY772	10
48	Afatinib	-32.72	1840	Ref.	2	ASP831(2.08), GLN767(3.03)	GLU738, ASN818, MET742, LYS721, LEU820, VAL702, LEU694, PRO770, LEU768, ALA719	12

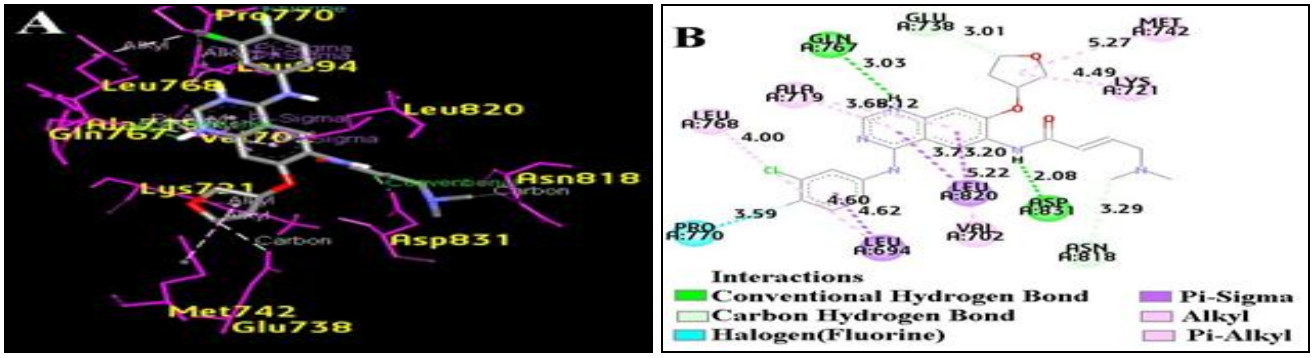

FIG. 5: DOCKING INTERACTIONS BETWEEN AFATINIB AND EGFR (1M17). (A) 3D- INTERACTIONS (B) 2D-INTERACTIONS

C21 **Fig. 6** forms two conventional hydrogen bonds with MET769; Pi-Cation interaction with LYS721, Pi-Sulphur interaction with MET742, Pi-Sigma interactions with LEU694, and Pi-Alkyl interactions with VAL702, ALA719, and LEU820. C42 **Fig. 7** forms a hydrogen bond with MET769; Pi-Cation interaction with LYS721, Pi-Sigma interaction with LEU694, and Pi-Alkyl interactions with LEU694, VAL702, LYS704, ALA719, LYS721, MET742, LEU768, PRO770, and LEU820. C47 **Fig. 8** forms hydrogen bonds with LYS721 and MET769, Pi-Anion interaction with ASP831, Pi-Sulphur interaction with CYS773, Pi-Sigma interactions with LEU820 and GLY772, and Pi-Alkyl interactions with VAL702, ALA719, LYS721, MET742, LEU764, and LEU820.

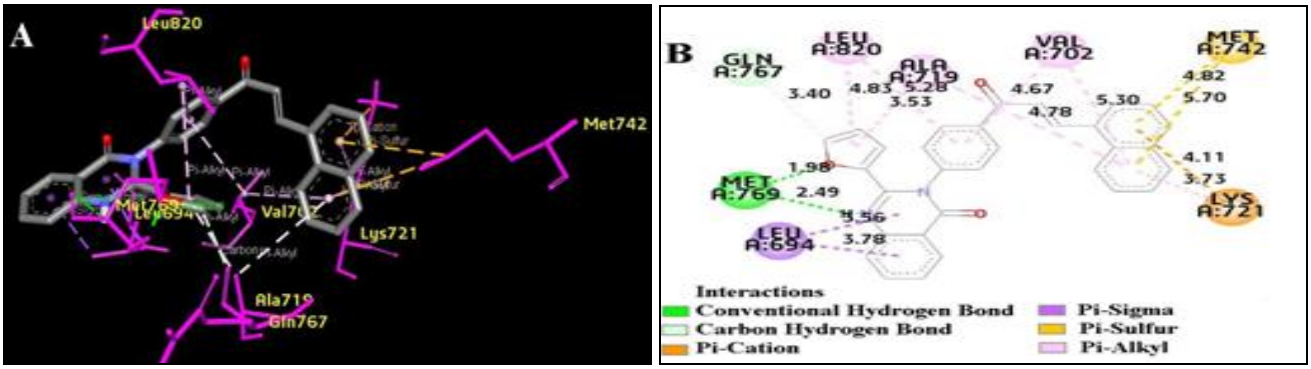

FIG. 6: DOCKING INTERACTIONS BETWEEN C21 AND EGFR (1M17). 3D- INTERACTIONS (B) 2D- INTERACTIONS

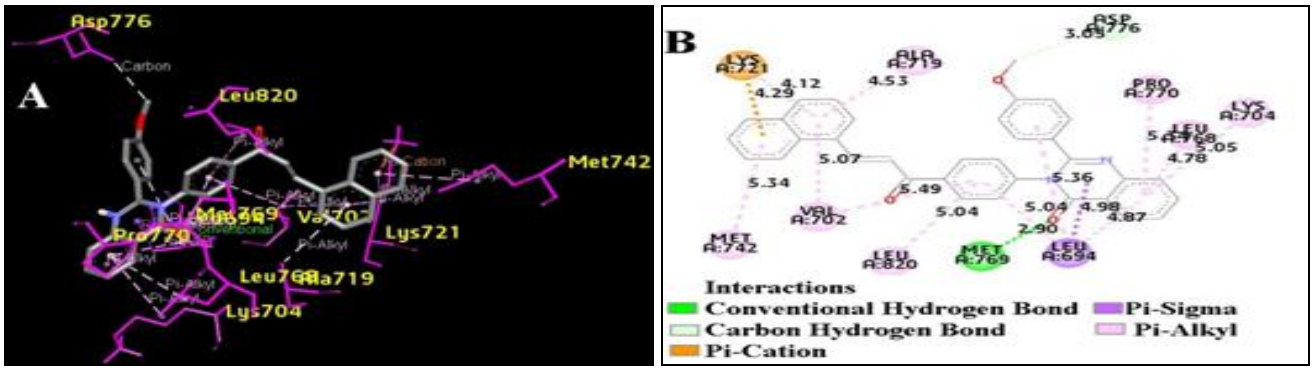

FIG. 7: DOCKING INTERACTIONS BETWEEN C42 AND EGFR (1M17). (A) 3D- INTERACTIONS (B) 2D- INTERACTIONS

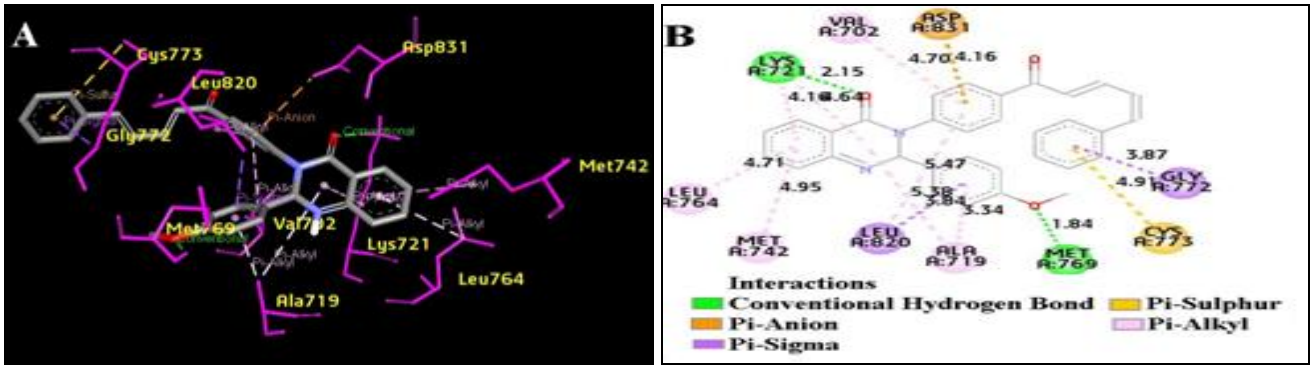

FIG. 8: DOCKING INTERACTIONS BETWEEN C47 AND EGFR (1M17). (A) 3D- INTERACTIONS (B) 2D- INTERACTIONS

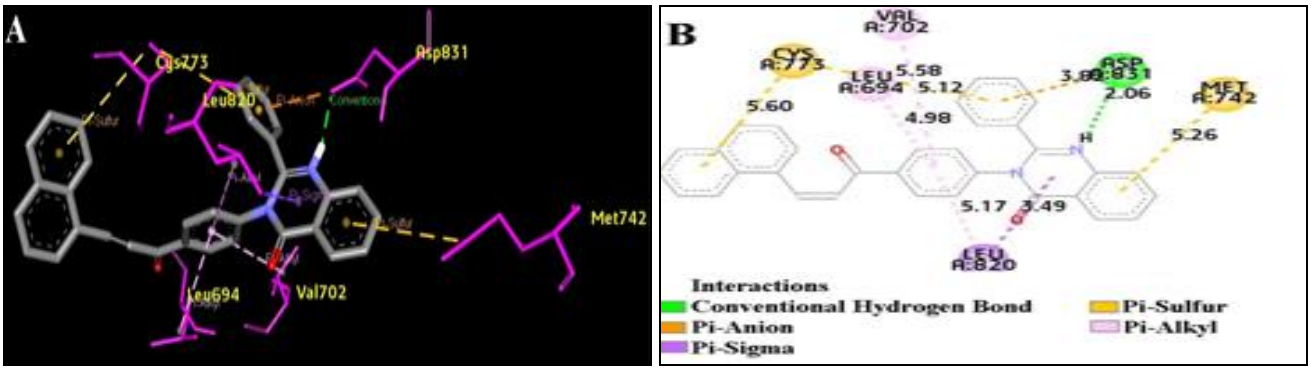

FIG. 9: DOCKING INTERACTIONS BETWEEN C10 AND EGFR (1M17). (A) 3D- INTERACTIONS (B) 2D- INTERACTIONS

C10 **Fig. 9** forms a hydrogen bond with ASP831, Pi-Anion interaction with ASP831, Pi-Sulphur interactions with MET742 and CYS773, Pi-Sigma interaction with LEU820 and Pi-Alkyl interactions with LEU694, VAL702, and LEU820.

C46 **Fig. 10** forms a hydrogen bond with ASP831, Pi-Cation interaction with LYS704, Pi-Anion interaction with ASP831, Pi-Sulphur interaction with MET742, Alkyl interaction with ARG817, and Pi-Alkyl interactions with LEU694, VAL702,

LYS721, LEU768, PRO770, CYS773, and LEU820. C26 **Fig. 11** forms a hydrogen bond with LYS721, Pi-Cation interaction with ARG817, Pi-Anion interaction with ASP831, Pi-Sigma interaction with ARG817, Alkyl interaction with LEU694, and Pi-Alkyl interactions with VAL702, ALA719, LYS721, MET742, LEU764, and LEU820. C24 **Fig. 12** forms a hydrogen bond with ASP831, Pi-sulphur interactions with MET742 and CYS773, Pi-Sigma interaction with LEU820, Alkyl interactions with ARG817 and CYS773 and Pi-Alkyl interactions with LEU694, VAL702, LYS721, CYS773, and LEU820. C44 **Fig. 13** forms a hydrogen bond with ASP831, Pi-Cation interactions with LYS704, Pi-Anion interaction with ASP831, Pi-Sulphur interaction with MET742 and, Pi-Alkyl interactions with LEU694, VAL702, LYS721, LEU768, PRO770 and LEU820.

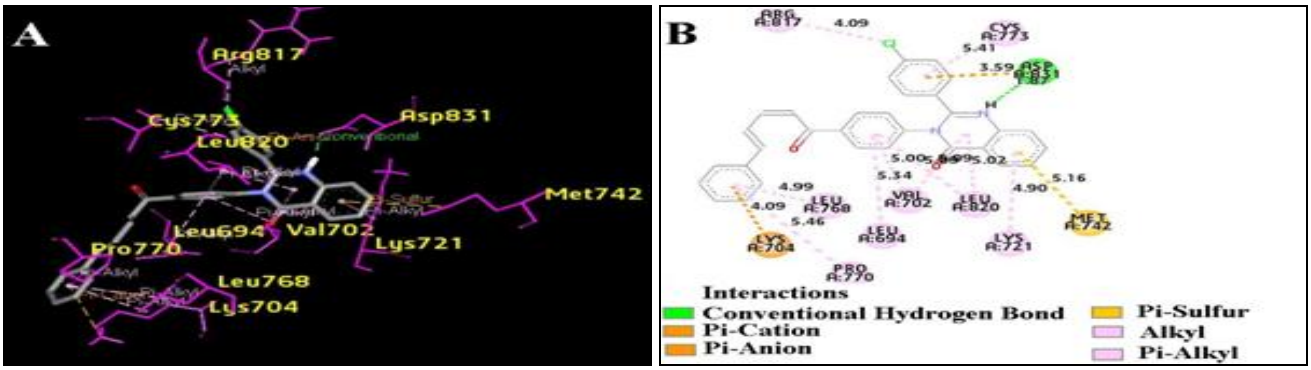

FIG. 10: DOCKING INTERACTIONS BETWEEN C46 AND EGFR (1M17). (A) 3D- INTERACTIONS (B) 2D- INTERACTION

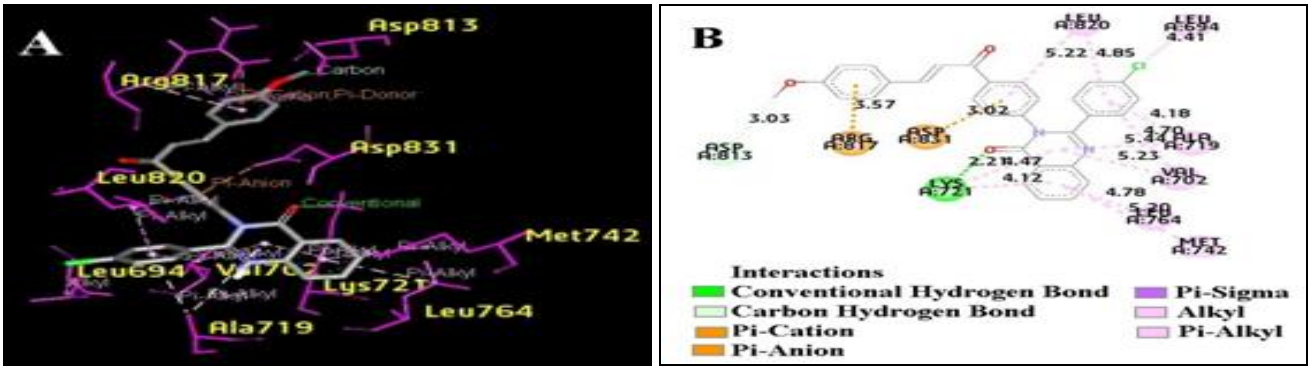

FIG. 11: DOCKING INTERACTIONS BETWEEN C26 AND EGFR (1M17). (A) 3D- INTERACTIONS (B) 2D- INTERACTION

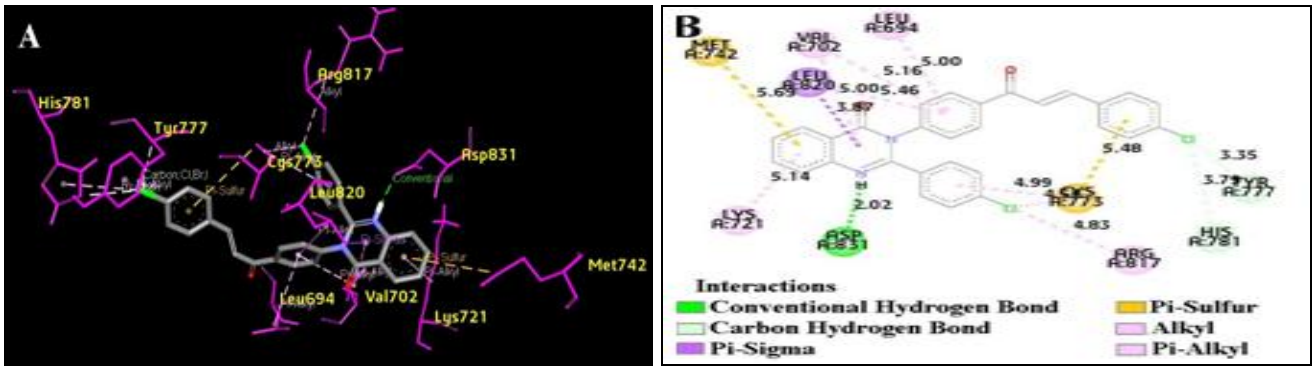

FIG. 12: DOCKING INTERACTIONS BETWEEN C24 AND EGFR (1M17). (A) 3D- INTERACTIONS (B) 2D- INTERACTIONS

C2 **Fig. 14** forms a hydrogen bond and Pi-Anion interaction with ASP831, Pi-Sulphur interaction with MET742, Alkyl interactions with LYS704 and LEU768 and Pi-Alkyl interactions with LEU694, VAL702, LYS 704, LYS721, LEU768, PRO770, and LEU820. C23 **Fig. 15** forms a hydrogen bond and Pi-Anion interaction with ASP831 and Pi Alkyl interactions with LEU694, VAL702, LYS 704, LYS721, LEU768, PRO770, and LEU820.

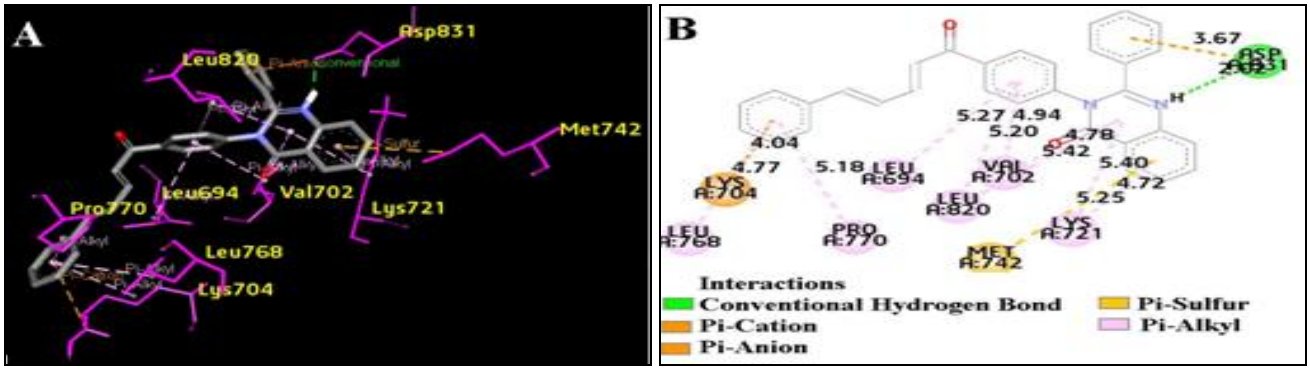

FIG. 13: DOCKING INTERACTIONS BETWEEN C44 AND EGFR (1M17). (A) 3D- INTERACTIONS (B) 2D- INTERACTIONS

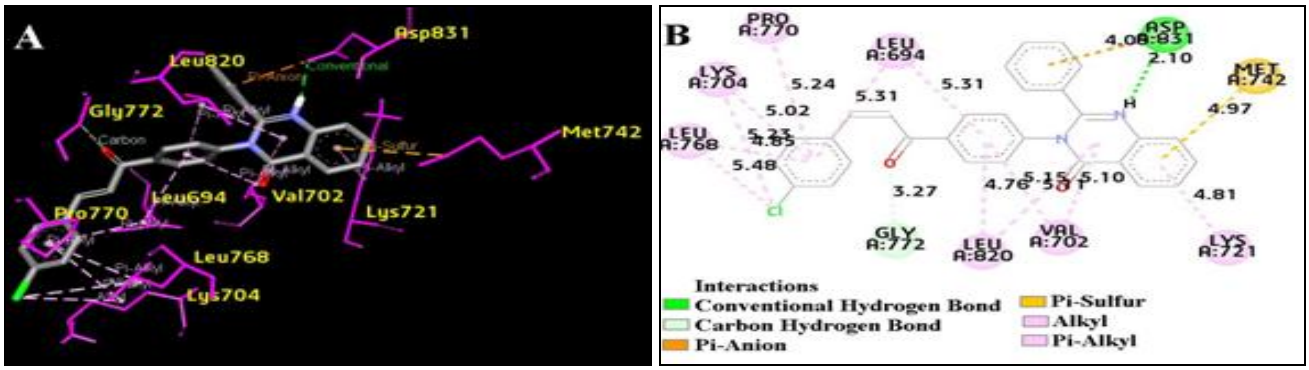

FIG. 14: DOCKING INTERACTIONS BETWEEN C2 AND EGFR (1M17). (A) 3D- INTERACTIONS (B) 2D- INTERACTION

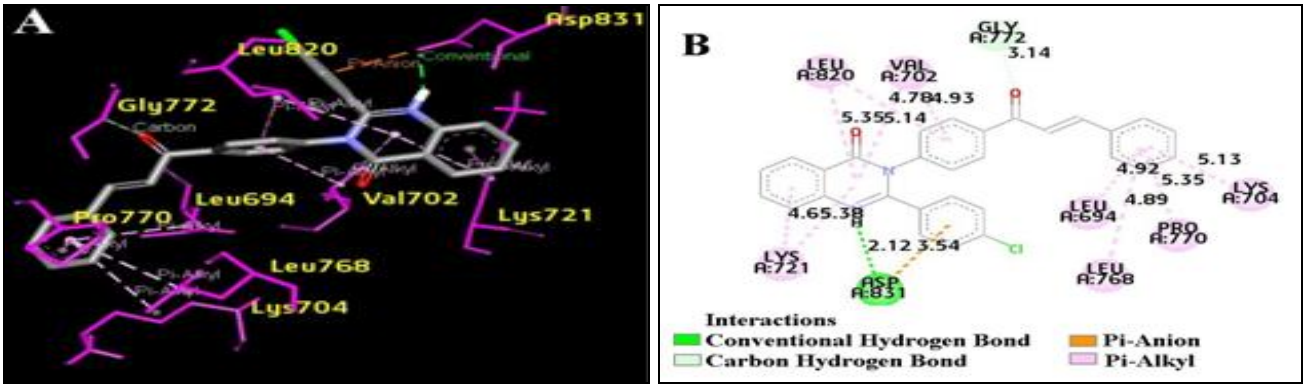

FIG. 15: DOCKING INTERACTIONS BETWEEN C23 AND EGFR (1M17). (A) 3D- INTERACTIONS (B) 2D- INTERACTIONS

CONCLUSION: The docking analysis reveals that the designed 2-arylquinazolin-4-one incorporated chalcones, are satisfactory scaffolds for EGFR (1M17) inhibition. It was observed that the amino acid residues ASP831, CYS773, LYS721, and MET 769 were important for H-bonding interactions. LYS721, LYS704, and ARG817 were important for pi-cation interactions. For pi-anion interaction, ASP831 was important, and for pi-sulphur interactions, MET742 and CYS773 were important. The amino acid residues LEU820, VAL702, MET742, ALA719, PRO770, LYS704, LEU768, LEU764, and LEU694 were important for pi-alkyl interactions. Hence, the study gives molecular insight into the binding process of the designed quinazolinones with the target EGFR protein (1M17). Lower binding energies, Lipinski compliance, good human intestinal as well as blood-brain barrier absorption, non-carcinogenicity, and non-mutagenicity of the designed ligands prompt the research to move on for the synthesis of *in-silico* potent EGFR inhibitors and carrying out the *in-vitro* assays to confirm their potency. Hence, the present research gives momentum to the discovery of low molecular weight novel EGFR inhibitors to treat advanced non-small-cell lung cancer (NSCLC) with a comparatively better prognosis.

ACKNOWLEDGMENTS: Nil

CONFLICTS OF INTEREST: The authors declare that they have no conflicts of interest.

REFERENCES:

1. Patidar K, Panwar U, Vuree S, Jajoriya S, Kaur MS, Nayarisseri A and Singh SK: An *In-silico* approach to identify high affinity small molecule targeting m-TOR inhibitors for the clinical treatment of breast cancer. Asian Pac J Cancer Prev 2019; 20(4): 1229-41.
2. Prada-Gracia D, Huerta-Yépez S and Moreno-Vargas LM: Application of computational methods for anticancer drug discovery, design and optimization. Bol Med Hosp Infant Mex 2016; 73(6): 411-23.
3. Bray F, Ferlay J, Soerjomataram I, Siegel RL, Torre LA and Jema A: Global cancer statistics 2018: GLOBOCAN estimates of incidence and mortality worldwide for 36 cancers in 185 countries. CA Cancer J Clin 2018; 68(6): 394-024.
4. Prabhakar CN: Epidermal growth factor receptor in non-small cell lung cancer. Transl Lung Cancer Res 2015; 4(2): 110-18.
5. Bao SM, Hu QH, Yang WT, Wang Y, Tong YP and Bao WD: Targeting epidermal growth factor receptor in non-small-cell-lung cancer: Current state and future perspective. Antic Agents Med Chem 2019; 19(8): 984-91.
6. Martinez-Marti A, Navarro A and Felip E: Epidermal growth factor receptor first generation tyrosine-kinase inhibitors. Transl Lung Cancer Res 2019; 8(3): 235-46.
7. Santarpia M, Altavilla G, Pitini V and Rosell R: Personalized treatment of early-stage non- small-cell lung cancer: The challenging role of EGFR inhibitors. Future Oncology 2015; 11(8): 1259-74.
8. Soria JC, Felip E, Cobo M, Lu S, Syrigos K, Lee KH, Göker E, Georgoulias V, Li W, Isla D, Guclu SZ, Morabito A, Min YJ, Ardizzoni A, Gadgeel SM, Wang B, Chand VK and Goss GD: Afatinib versus erlotinib as second-line treatment of patients with advanced squamous cell carcinoma of the lung (LUX-lung 8): An open-label randomised controlled phase 3 trial. Lancet Oncol 2015; 16 (8): 897-07.
9. Sharma N and Graziano S: Overview of the LUX-lung clinical trial program of afatinib for non-small cell lung cancer. Cancer Treat Rev 2018; 69: 143-51.
10. Stamos J, Sliwkowski MX and Eigenbrot C: Structure of the epidermal growth factor receptor kinase domain alone and in complex with a 4-anilinoquinazoline inhibitor. J Biol Chem 2002; 277(48): 46265-72.
11. Daina A, Michielin O and Zoete V: Swiss ADME: A free web tool to evaluate pharmacokinetics, drug-likeness and medicinal chemistry friendliness of small molecules. Sci Rep 2017; 7: 42717-29.
12. Lipinski CA: Rule of five in 2015 and beyond: Target and ligand structural limitations, ligand chemistry structure and drug discovery project decisions. Advanced Drug Delivery Reviews 2016; 101: 34-41.
13. Forli S, Huey R, Pique ME, Sanner MF, Goodsell DS and Olson AJ: Computational protein-ligand docking and virtual drug screening with the Auto Dock suite. Nat Protoc 2016; 11(5): 905-19.
14. El-Hachem N, Haibe-Kains B, Khalil A, Kobeissy FH and Nemer G: Auto Dock and Auto Dock tools for protein-ligand docking: Beta-site amyloid precursor protein cleaving enzyme 1(BACE1) as a case study. Methods Mol Biol 2017; 1598: 391-03.
15. Hameed A, Rashida MA, Uroos M, Ali SA, Arshia, Ishtiaq M and Khan KM: Quinazoline and quinazolinone as important medicinal scaffolds: A comparative patent review (2011-2016). Expert Opinion on Therapeutic Patents 2018; 28(4): 281-97.
16. OuYang Y, Zou W, Peng L, Yang Z, Tang Q, Chen M, Jia S, Zhang H, Lan Z, Zheng P and Zhu W: Design, synthesis, antiproliferative activity and docking studies of quinazoline derivatives bearing 2,3-dihydro-indole or 1,2,3,4-tetrahydroquinoline as potential EGFR inhibitors. European J of Medicinal Chemistry 2018; 154: 29-43.
17. Zayed MF, Ahmed S, Ihmaid S, Ahmed HEA, Rateb HS and Ibrahim SRM: Design, synthesis, cytotoxic evaluation and molecular docking of new fluoroquinazolinones as potent anticancer agents with dual EGFR kinase and tubulin polymerization inhibitory effects. Int J Mol Sci 2018; 19(6): 1731-47.
18. 18. Yu CH, Chou CC, Tu HF, Huang WC, Ho YY, Khoo KH, Lee MS and Chang GD: Antibody-assisted target identification reveals afatinib, an EGFR covalent inhibitor, down-regulating ribonucleotide reductase. Oncotarget 2018; 9(30): 21512-529.
19. Zhuang C, Zhang W, Sheng C, Zhang W, Xing C and Miao Z: Chalcone: A privileged structure in medicinal chemistry. Chem Rev 2017; 117(12): 7762-10.
20. Chhajed SS, Sonawane SS, Upasani CD, Kshirsagar SJ and Gupta PP: Design, synthesis and molecular modeling studies of few chalcone analogues of benzimidazole for epidermal growth factor receptor inhibitor in search of useful anticancer agent. Com Biol Chem 2016; 61: 138-44.
21. Khan I, Garikapati KR, Setti A, Shaik AB, Makani VK, Shareef MA, Rajpurohit H, Vangara N, Bhadra MP, Kamal A and Kumar CG: Design, synthesis, in-silico pharmacokinetics prediction and biological evaluation of 1,4-dihydroindeno[1,2-c]pyrazole chalcone as EGFR /Akt pathway inhibitors. European Journal of Medicinal Chemistry 2019; 163: 636-48.
22. Fathi MAA, Abd El-Hafeez AA, Abdelhamid D, Abbas SH, Montano MM and Abdel-Aziz M: 1, 3, 4-oxadiazole/chalcone hybrids: Design, synthesis, and inhibition of leukemia cell growth and EGFR, Src, IL-6 and STAT3 activities. Bioorg Chem 2019; 84: 150-63.
23. Abdelbaset MS, Abdel-Aziz M, Ramadan M, Abdelrahman MH, Abbas Bukhari SN, Ali TFS and Abuo-Rahma GEA: Discovery of novel thienoquinoline-2-carboxamide chalcone derivatives as antiproliferative EGFR tyrosine kinase inhibitors. Bioorg Med Chem 2019; 27(6): 1076-86.

How to cite this article:
Arora PK Kumar S and Bansal SK: Docking - based virtual screening of lipinski compliant 2 -arylquina-zolin - 4 - one derivatives: a momentum to the discovery of novel egfr inhibitors. Int J Pharm Sci & Res 2021; 12(3): 1699-12. doi: 10.13040/IJPSR.0975-8232. 12(3).1699-12.